Available online at www.sciencedirect.com
ScienceDirect
International Journal of Mass Spectrometry 268 (2007) 1–7
International Journal of Mass Spectrometry
www.elsevier.com/locate/ijms

Electrophilic properties of common MALDI matrix molecules

T.P. Lippa [a,*], S.N. Eustis [b], D. Wang [b], K.H. Bowen [b,*]

[a] *Applied Physics Laboratory, Johns Hopkins University, Laurel, MD 20723, United States*
[b] *Department of Chemistry, Johns Hopkins University, Baltimore, MD 21218, United States*

Received 22 June 2007; received in revised form 26 July 2007; accepted 27 July 2007
Available online 2 August 2007

Abstract

The negative ion photoelectron spectra of the following MALDI matrix molecules have been measured: 3-carboxypyridine (nicotinic acid), 2,5-dihydroxybenzoic acid (DHB), 3,5-dimethoxy-4-hydroxycinnamic acid (sinapinic acid), 2,6-dihydroxyacetophenone (DHAP), 3-(4-hydroxy-3-methoxyphenyl)-2-propenoic acid (ferulic acid), 3-hydroxy-2-pyridinecarboxylic acid (3HPA), and 2,6-pyridinedicarboxylic acid (dipicolinic acid). Adiabatic electron affinities and vertical detachment energies were extracted from these spectra and reported. In addition, electron affinities were calculated for DHAP, ferulic acid, dipicolinic acid and sinapinic acid. Photoelectron spectra were also measured for the dimer anions of DHB and nicotinic acid and for the fragment anion in which alpha-cyano-cinnamic acid had lost a CO_2 unit. Together, these results augment the database of presently available electrophilic data on common matrix molecules along with some of their dimers and fragments.

Keywords: MALDI; Matrix compound; Photoelectron spectroscopy; Negative ion; Electron affinity

1. Introduction

Since the inception of the matrix-assisted laser desorption-ionization (MALDI) technique [1–4], investigators have attempted to elucidate the mechanisms which are at work in the MALDI process. Attempts to interpret, predict, and thereby understand, MALDI mass spectra require thermochemical data about both the matrix and the analyte molecules [5–7]. As might be expected, a substantial portion of the effort to date has focused on ionization potentials [8,9] and proton affinities [8,10,11] of matrix molecules, both of which are central to understanding the role of cations in MALDI mechanisms. When it comes to anions, however, there is much less energetic information available about commonly used matrix molecules. Gas phase basicity values have been measured [12–14], and some electron affinity values have been calculated [8], but there is a dearth of experimentally determined electron affinity values in the literature.

In the present work, we report adiabatic electron affinities (EA_a) and vertical detachment energies (VDE), measured via anion photoelectron spectroscopy, for seven common MALDI matrix compounds, two of their dimers, and a selected molecular fragment. Adiabatic electron affinities and vertical detachment energies are the electrophilic counterparts to adiabatic and vertical ionization potentials, and as such they are central to understanding the fate of electrons, the role that matrix anions play in the ionization process in MALDI generally, and anion formation in negative ion MALDI in particular. To facilitate more complete comparisons, we also calculated electron affinity and ionization potential values for those species in this study whose theoretical values had not been previously reported. Thus, this paper presents a compilation of previously unavailable (experimentally and theoretically determined) electrophilic data on common matrix molecules which, it is hoped, will support a further understanding of the MALDI process and aid in the prediction and description of ions formed by this technique.

2. Experimental and computational methods

Negative ion photoelectron spectroscopy was used measure the electron affinities and vertical detachment energies of several common matrix molecules and their anions. Anion photoelectron spectroscopy is conducted by crossing a mass-selected beam of negative ions with a fixed-frequency photon beam and energy-analyzing the resultant photodetached electrons. The

* Corresponding authors.
E-mail addresses: timothy.lippa@jhuapl.edu (T.P. Lippa), kbowen@jhu.edu (K.H. Bowen).

1387-3806/$ – see front matter © 2007 Elsevier B.V. All rights reserved.
doi:10.1016/j.ijms.2007.07.019

photodetachment process is governed by the relationship,

$$h\nu = \mathrm{EBE} + \mathrm{EKE} \quad (1)$$

where $h\nu$ is the photon energy, EBE the electron binding energy, and EKE is the electron kinetic energy. Essentially, the photon energy is sub-divided into the transition energy needed to take the anion to a particular vibronic state of its neutral counterpart, i.e., EBE, and the kinetic energy of the electron, i.e., EKE. Fig. 1 illustrates the energetics of photodetachment transitions. Because photodetachment is a fast process, the essentially instantaneous Franck-Condon overlap of anion and neutral wavefunctions is reflected in the vertical detachment energy, VDE. When the structures of the anion, X^-, and its corresponding neutral, X are different (as in Fig. 1), the VDE is the EBE of the maxima in the broadened photoelectron spectral profile, and as such, it is a well-defined quantity.

When there is Franck-Condon overlap between the lowest vibrational level of the anion (v'') and the lowest vibrational level its corresponding neutral (v'), the photoelectron spectrum carries information about the adiabatic (thermodynamic) electron affinity of the neutral species. When the spectral profile is vibrationally resolved, an assignment of the spectrum can identify the $v''=0 \rightarrow v'=0$ transition. For this transition, its EBE value is equal to the adiabatic electron affinity, EA_a. When the profile is unresolved, however, the determination of EA_a is more approximate. If the anions were to be cold, i.e., if only $v''=0$ were occupied, then the low EBE threshold value of the spectrum would equal the EA_a value. But because anions are generated with finite internal temperatures, the first few vibrational levels of anions may also occupied, leading to some degree of photoelectron intensity at EBE values less than that corresponding to the EA_a, i.e., hot bands. Thus, in order to extract reasonable estimates of EA_a values from unresolved photoelectron spectral profiles (bands), one needs to calibrate the procedure by which this is done. Below, we present a procedure for performing this calibration in the case of relatively similar matrix molecular anions.

The apparatus consists of a source for generating anions, a magnetic sector for mass analysis and mass selection, an argon ion laser operated intra-cavity as the photon source, and a hemispherical electron energy analyzer. The mass analyzer/selector has a mass resolution of ~500, and the electron energy analyzer has a resolution of 28 meV. All photoelectron spectra reported here were recorded with 2.540 eV photons and calibrated against the photoelectron spectrum of O^- [15,16]. Our apparatus has been described previously [17].

Negative ions of selected matrix molecules and their dimers were generated in a supersonic expansion, nozzle-ion source which was biased at −500 V. Samples of the matrix materials of interest were placed inside the stagnation chamber of the source and heated to temperatures ranging between 150 and 220 °C in order to partially vaporize them. The resulting vapor was then co-expanded with argon (5–25 psia) through a ~100 μm orifice into vacuum. Negative ions were formed by injecting electrons from a biased filament into the expanding jet, where a microplasma was formed with the help of an external magnetic field. Negative ions were then extracted into the beam-line of the apparatus and subsequently mass-selected so that the anions of interest could be photodetached.

Computations to determine the values of the electron affinities, vertical detachment energies, and ionization potentials of selected matrix molecules were performed with Gaussian 03 [18] following the density functional theoretical methodology (B3LYP/6-31 + G(d,p)/6-311 ++ G(2d,2p)) utilized by Bourcier and Hoppilliard [8].

3. Results and discussion

3.1. Monomers

The photoelectron spectra of the parent molecular anions of nicotinic acid, DHB (2,5-dihydroxybenzoic acid), sinapinic acid, DHAP (2,6-dihydroxyacetophenone), ferulic acid, 3HPA (3-hydroxy-2-pyridinecarboxylic acid), and dipicolinic acid are presented in Figs. 2–8. While the photoelectron spectra of the nicotinic acid anion and the DHB anion show vibrational structure, the spectra of the other five exhibit only broad, unstructured

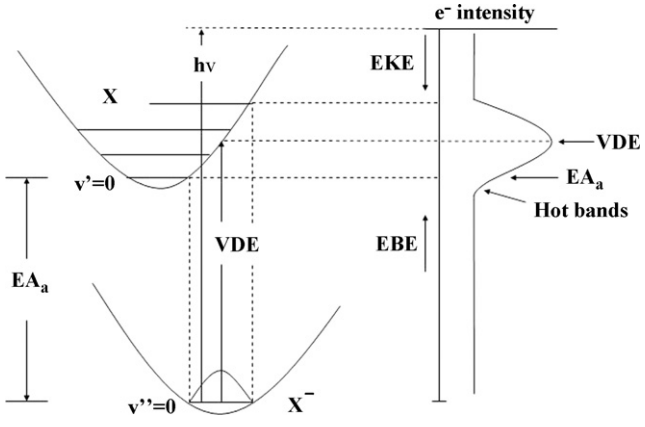

Fig. 1. Schematic diagram showing the energetics of the photodetachment process.

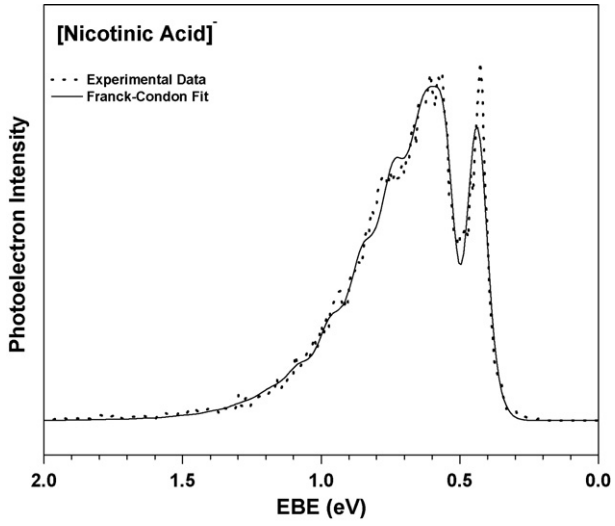

Fig. 2. Photoelectron spectrum of the nicotinic acid anion along with its Franck-Condon fit.

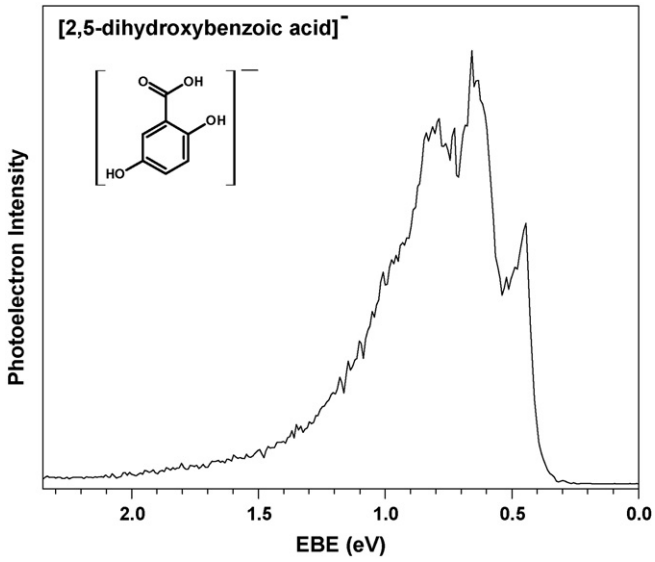

Fig. 3. Photoelectron spectrum of the 2,5-dihydroxybenzoic acid anion.

bands. In all cases, vertical detachment energies are taken to be the EBE values of the fitted maxima of their spectral profiles, whether they were vibrationally structured or not. Sinapinic acid and ferulic acid both have similar spectral profiles with a pronounced plateau on the high electron binding energy side of the peak. These bands, though unresolved, are indicative of a transition from the molecular anion to the first excited state of the neutral molecule. In the cases of the spectra of nicotinic acid anion and DHB anion, adiabatic electron affinities were determined by identifying the ($v'' = 0 \rightarrow v' = 0$) origin peak, which in both cases is the lowest EBE peak in their spectra. This assignment of the origin transition was reinforced by conducting a Franck-Condon analysis on the nicotinic acid anion spectrum. The Franck-Condon fit is shown superimposed onto the experimental photoelectron spectrum of the nicotinic acid anion in Fig. 2 and the parameters of the simulation are presented in Table 1. In addition to confirming that the lowest EBE peak is

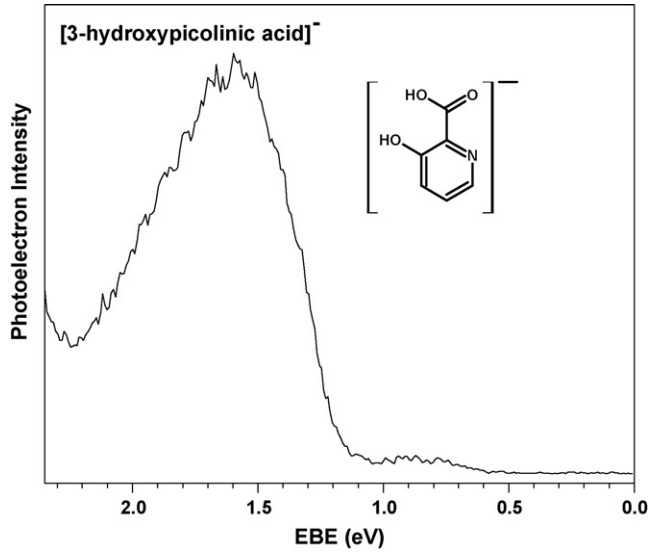

Fig. 4. Photoelectron spectrum of the 3-hydroxypicolinic acid anion.

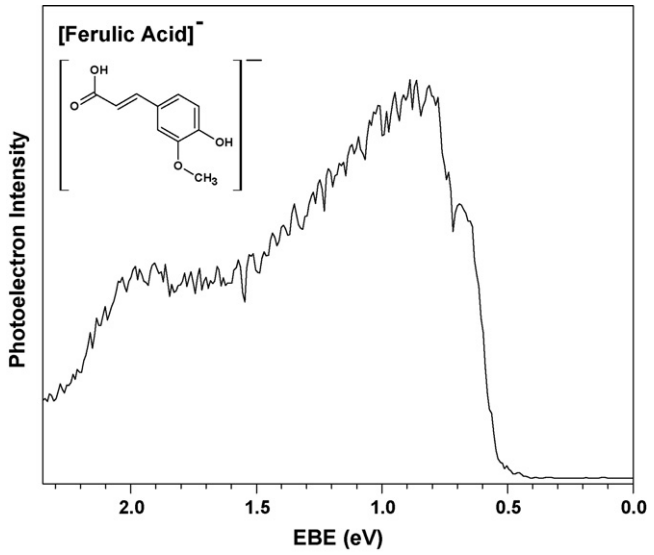

Fig. 5. Photoelectron spectrum of the ferulic acid anion.

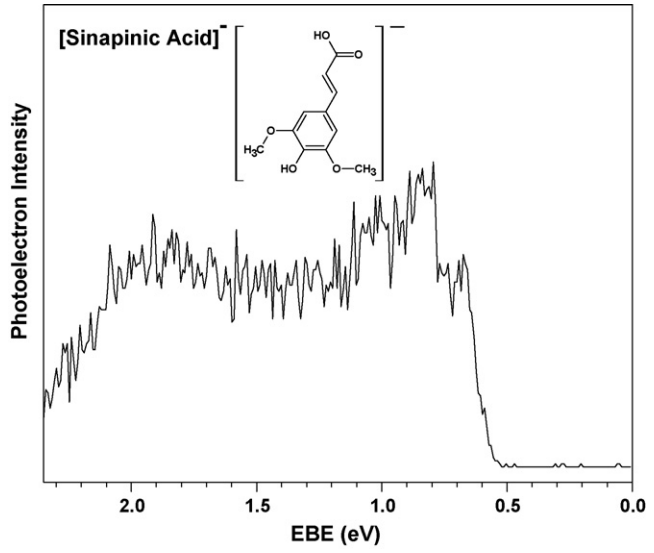

Fig. 6. Photoelectron spectrum of the sinapinic acid anion.

Table 1
Parameters obtained from the Franck-Condon fit of the nicotinic acid photoelectron spectrum

$\nu_{(0,0)}$ (eV)	0.438
Temperature (K)	263
Mode 1	
Displacement ($A(\mu)^{1/2}$)	0.323
ω_e (anion, cm^{-1})	588
ω_e (neutral, cm^{-1})	936
Mode 2	
Displacement ($A(\mu)^{1/2}$)	−0.139
ω_e (anion, cm^{-1})	3197
ω_e (neutral, cm^{-1})	1447

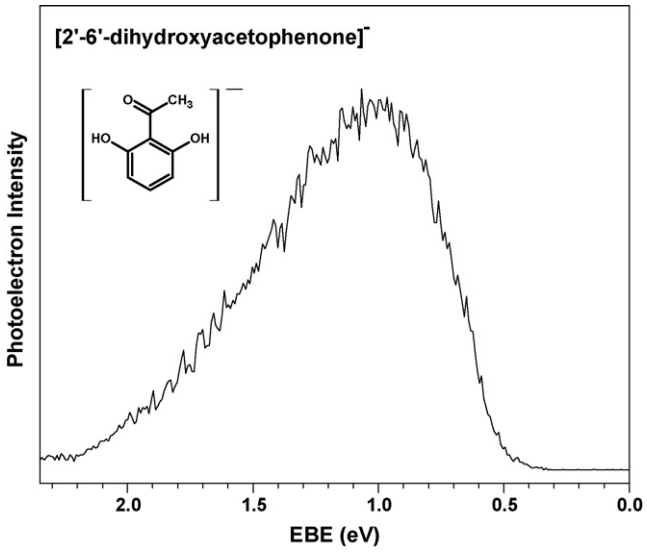

Fig. 7. Photoelectron spectrum of the 2′,6′-dihydroxyacetophenone anion.

indeed due to the origin transition, this analysis also indicated that the internal temperature of the anion was ∼260 K. More importantly, the assignment of this spectrum provided a calibration procedure for estimating the adiabatic electron affinities for the matrix molecules with unstructured spectra. If the spectrum of nicotinic acid anion had been unstructured, its origin transition would have been located at a point on the low EBE side of the spectral profile that was ∼23% of the peak intensity maximum. Because all of the molecules under study here are of similar size and complexity, because three of the five unstructured spectra have similar overall profiles, and because all anions studied here were generated under similar source conditions, we have used this *ad hoc* procedure to estimate adiabatic electron affinities in each case. Table 2 presents the adiabatic electron affinities and vertical detachment energies determined from these measurements. For comparison, calculated values of adiabatic electron affinities are also shown.

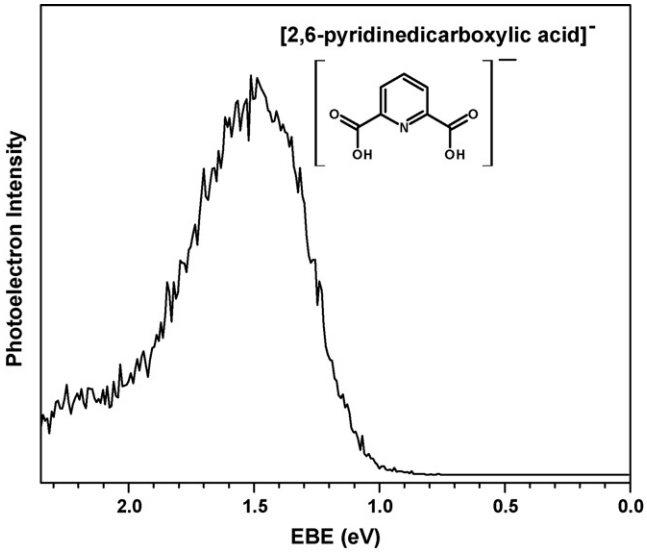

Fig. 8. Photoelectron spectrum of the 2,6-pyridinedicarboxylic acid anion.

These energetic data lead to several observations and comments. (1) Previous studies of electron attachment to nicotinic acid did not observe its parent anion, prompting investigators to suspect that it is unstable [19]. In the present studies, however, we have conclusively observed it and measured its (positive) EA_a value, showing that it is stable. (2) The seven monomers we have studied fall into two categories in regard to the size of their electron affinities values. Both dipicolinic acid and 3-hydroxy-2-pyridinecarboxylic acid have EA_a values which are larger than 1 eV, while the other five possess smaller EA_a values. (3) Zenobi and Knochenmuss have pointed out that a given matrix material can often provide both positive and negative analyte ions [20]. They suggest that one pathway for this apparent correlation may be primary ionization of 2 M (due to the two photon excitation of matrix molecule pairs) to yield cations, M^+ and anions, M^-, i.e.,

$$2M \xrightarrow{nh\nu} M^+ + M^- \quad (2)$$

If so, this would require that a threshold energy of IP(M)–EA(M) be provided by the two photon process. Nitrogen lasers, commonly used as excitation sources in MALDI, have a two-photon energy of 7.36 eV. Additionally, both frequency tripled (355 nm) and quadrupled (266 nm) YAG lasers have been demonstrated to be effective. These lasers have two photon energies of 9.32 and 6.99 eV, respectively. Table 3 provides a tabulation of IP(M), EA(M), and IP(M)–EA(M) values for the matrix systems that we studied. While some of the tabulated IP(M)–EA(M) values fall below the two-photon energies of the lasers, making this mechanism feasible, others fall above it, putting the same mechanism energetically out of reach. Nicotinic acid, developed for the 266 nm wavelength [21] has a disproportionation energy that falls below the 266 nm two photon energy. Thus, while this mechanism for the matrix monomers may well contribute, along with others, to the correlated formation of positive and negative ions in many MALDI matrix materials, consideration must also be given to the matrix clusters known to exist in the MALDI plume. This is discussed below.

3.2. Dimers

Figs. 9 and 10 show the photoelectron spectra of the nicotinic acid dimer anion and the 2,5-dihydroxybenzoic acid (DHB) dimer anion. As dimer anions, the spectra of both species have lost the vibrational structure that they exhibited as monomer anions. Values for VDE and EA_a were extracted from their spectra using the same procedure described above for their monomers (see Table 2). In comparison to their monomers, VDE and EA_a values for these dimers increased by significantly more than an eV, reflecting the enhanced stability of these dimer anions with respect to electron loss. In fact, it can be generally expected that clustering will greatly increase the stability of dimers and larger sized cluster anions. Knochenmuss and Zhigilei have detailed molecular dynamics simulations that demonstrate substantial clustering early in the MALDI expansion [22] and clusters in MALDI plumes have been seen experimentally [23]. It is likely that cluster anions are significant players in the ion

Table 2
Experimental and calculated data for the matrix compounds studied

Matrix (common)	Matrix (IUPAC)	VDE (eV) (expt.)[b]	EA (eV) (expt.)[b]	EA (eV) (calc.)
Nicotinic acid	3-Carboxypyridine	0.63	0.44	0.61[a]
DHB	2,5-Dihydroxybenzoic acid	0.73	0.42	0.56[a]
Sinapinic acid	3,5-Dimethoxy-4-hydroxycinnamic acid	0.92	0.59	0.69[b]
DHAP	2,6-Dihydroxyacetophenone	1.05	0.59	0.42[b]
Ferulic acid	3-(4-Hydroxy-3-methoxyphenyl)-2-propenoic acid	0.92	0.58	0.82[b]
3HPA	3-Hydroxy-2-pyridinecarboxylic acid	1.61	1.24	1.0[a]
Dipicolinic acid	2,6-Pyridinedicarboxylic acid	1.50	1.17	1.40[b]
[CHCA – CO_2]	3-(4-Hydroxy-phenyl)-acrylonitrile	0.88	0.54	0.63[b]
$(Nicotinic\ acid)_2$	$(3\text{-Carboxypyridine})_2$	2.07	1.62	–
$(DHB)_2$	$(2,5\text{-Dihydroxybenzoic acid})_2$	2.15	1.72	–

[a] [8].
[b] This work.

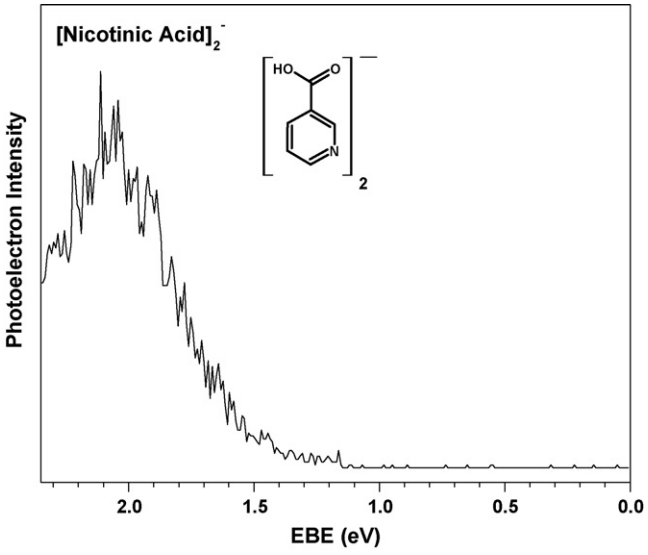

Fig. 9. Photoelectron spectrum of the nicotinic acid dimer anion.

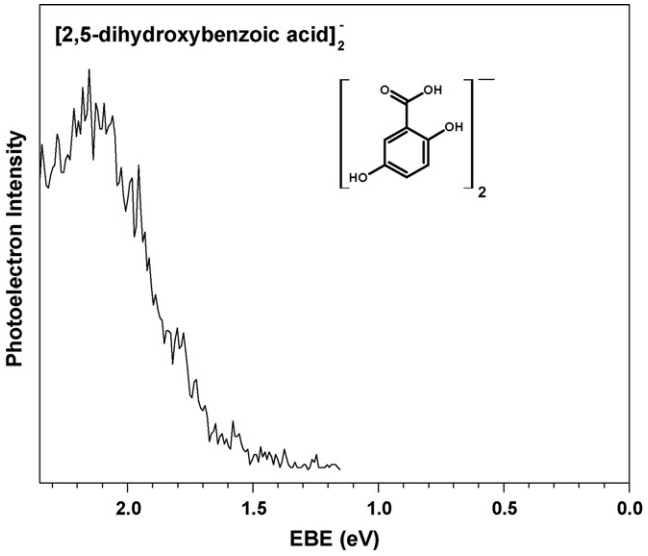

Fig. 10. Photoelectron spectrum of the 2,5-dihydroxybenzoic acid dimer anion.

chemistry of both irradiated matrices and their resulting plumes [13,21,22]. With respect to the disproportionation reactions discussed above, the situation for the energetics of the process are much more favorable when we begin to consider dimers and larger clusters. In comparison to the parent monomer, DHB ionization potential reductions have been experimentally [9] and theoretically [24] observed for DHB clusters. These reductions continue as the cluster sizes increase until an estimated bulk limit of 7.82 eV is reached [9]. We anticipate the electron affinity to increase as clusters continue to larger sizes, asymptotically approaching the electron affinity of the condensed phase. However, we cannot estimate the bulk value from the monomer and dimer alone. If the dimer is considered, the IP-EA for a dimer pair results in an energy of 6.22 eV, well below the two photon threshold for any of the UV lasers listed above. The importance of clusters in the ion energetics of the MALDI plume continues to become more apparent and the information here supports the possibility of disproportionation, especially early in the MALDI plume where clusters are known to exist.

Table 3
Parameters relevant to the two-photon disproportionation process

Molecule	IP (eV)	EA (eV, expt.)[e]	(IP-EA) (eV)
Nicotinic acid	9.38[c]	0.44	8.94
DHB	8.05[b]	0.42	7.63
Sinapinic acid	7.72[g]	0.59	7.13
DHAP	8.43[e]	0.59	7.84
Ferulic acid	7.82[a]	0.58	7.24
3HPA	8.95[d]	1.24	7.71
Dipicolinic acid	9.71[e]	1.17	8.54
CHCA – CO_2	8.22[e]	0.54	7.68
$(Nicotinic\ acid)_2$	–	1.62	–
$(DHB)_2$	7.94[f]	1.72	6.22

[a] [27].
[b] [28].
[c] [29].
[d] [8].
[e] This work.
[f] [9].
[g] [31].

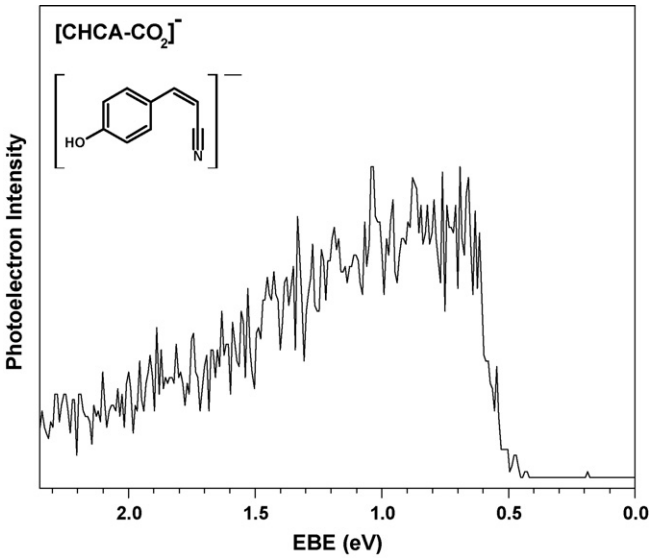

Fig. 11. Photoelectron spectrum of the fragment anion of α-cyano-4-hydroxycinnamic acid in which a carbon and two oxygen atoms have been loss.

3.3. Fragment ions

While attempting to generate parent anions of α-cyano-4-hydroxycinnamic acid (CHCA), we instead observed high intensities of its fragment anion $[CHCA - CO_2]^-$, and only a weak signal for the parent. Because this fragment ion was seen in previous MALDI studies of CHCA [26,27], we recorded its photoelectron spectrum, and it is presented in Fig. 11. There, one sees a steep onset of signal on the low EBE side of the spectral profile. Values of VDE and EA_a were estimated using the procedures described above, and these are tabulated in Table 2.

Secondary ion–molecule reactions are recognized as being important pieces of the bigger picture in MALDI ion formation, and fragment ions are examples of secondary ions that can be formed [6,28,29]. In fact, the appearance of some ions is more a function of secondary ion formation than it is of primary ion formation [6,25]. Thus, it is not enough to have energetic data only about the parent ions of matrix molecules; energetic information about fragment ions is also required.

4. Conclusion

In order to fully describe MALDI processes, access to energetic parameters for all participating species, including clusters and fragments, is required. Here, we have contributed to this database by determining electrophilic properties for several matrix molecules, their dimers and their fragments. It is clear, however, that information on the matrix molecules is not enough. One must also have comparable energetic information on analytes. Much ion chemistry in MALDI is governed by differences between the ionization potentials of matrix molecules and analytes in cation mode and by differences between the electron affinities of matrix molecules and analytes in anion mode [25,30]. The data presented here can be incorporated into quantitative models for the MALDI process such as those developed by Knochenmuss and Zhigilei [22,31] Furthermore, knowing the electron affinities of matrix species will help facilitate extension of these types of models to the formation of negative ions in MALDI.

Acknowledgment

This material is based upon work supported by the National Science Foundation under Grant No. CHE-0517337.

References

[1] M. Karas, D. Bachmann, F. Hillenkamp, Anal. Chem. 57 (1985) 2935.
[2] M. Karas, D. Bachmann, U. Bahr, F. Hillenkamp, Int. J. Mass Spectrom. Ion Process. 78 (1987) 53.
[3] M. Karas, F. Hillenkamp, Anal. Chem. 60 (1988) 2299.
[4] K. Tanaka, H. Waki, Y. Ido, S. Akita, Y.T. Yoshida, Rapid Commun. Mass Spectrom. 2 (1988) 151.
[5] R. Zenobi, K. Breuker, R. Knochenmuss, E. Lehmann, E. Stevenson, Adv. Mass Spectrom. 15 (2001) 143.
[6] R. Knochenmuss, A. Stortelder, K. Breuker, R. Zenobi, J. Mass Spectrom. 35 (2000) 1237.
[7] K. Breuker, R. Knochenmuss, J. Zhang, A. Stortelder, R. Zenobi, Int. J. Mass Spectrom. 226 (2003) 211.
[8] S. Bourcier, Y. Hoppilliard, Int. J. Mass Spectrom. 217 (2002) 231.
[9] Q. Lin, R. Knochenmuss, Rapid Commun. Mass Spectrom. 15 (2001) 1422.
[10] R.D. Burton, C.H. Watson, J.R. Eyler, G.L. Lang, D.H. Powell, M.Y. Avery, Rapid Commun. Mass Spectrom. 11 (1997) 443.
[11] T.J.D. Jorgensen, G. Bojesen, H. Rahbek-Nielsen, Eur. Mass Spectrom. 4 (1998) 39.
[12] K. Breuker, R. Knochenmuss, R. Zenobi, Int. J. Mass Spectrom. 184 (1999) 25.
[13] K. Breuker, R. Knochenmuss, R. Zenobi, J. Am. Soc. Mass Spectrom. 10 (1999) 1111.
[14] R.J.J.M. Steenvoorden, K. Breuker, R. Zenobi, Eur. Mass Spectrom. 3 (1997) 339.
[15] M.J. Travers, D.C. Cowles, G.B. Ellison, Chem. Phys. Lett. 164 (1989).
[16] P.M. Dehmer, W.A. Chupka, J. Chem. Phys. 62 (1975) 4525.
[17] J.V. Coe, J.T. Snodgrass, C.B. Freidhoff, K.M. Mchugh, K.H. Bowen, J. Chem. Phys. 84 (1986) 618.
[18] Gaussian 03, Revision D.01, M.J. Frisch, G.W. Trucks, H.B. Schlegel, G.E. Scuseria, M.A. Robb, J.R. Cheeseman, J.A. Montgomery, Jr., T. Vreven, K.N. Kudin, J.C. Burant, J.M. Millam, S.S. Iyengar, J. Tomasi, V. Barone, B. Mennucci, M. Cossi, G. Scalmani, N. Rega, G.A. Petersson, H. Nakatsuji, M. Hada, M. Ehara, K. Toyota, R. Fukuda, J. Hasegawa, M. Ishida, T. Nakajima, Y. Honda, O. Kitao, H. Nakai, M. Klene, X. Li, J.E. Knox, H.P. Hratchian, J.B. Cross, V. Bakken, C. Adamo, J. Jaramillo, R. Gomperts, R.E. Stratmann, O. Yazyev, A.J. Austin, R. Cammi, C. Pomelli, J.W. Ochterski, P.Y. Ayala, K. Morokuma, G.A. Voth, P. Salvador, J.J. Dannenberg, V.G. Zakrzewski, S. Dapprich, A.D. Daniels, M.C. Strain, O. Farkas, D.K. Malick, A.D. Rabuck, K. Raghavachari, J.B. Foresman, J.V. Ortiz, Q. Cui, A.G. Baboul, S. Clifford, J. Cioslowski, B.B. Stefanov, G. Liu, A. Liashenko, P. Piskorz, I. Komaromi, R.L. Martin, D.J. Fox, T. Keith, M.A. Al-Laham, C.Y. Peng, A. Nanayakkara, M. Challacombe, P. M.W. Gill, B. Johnson, W. Chen, M.W. Wong, C. Gonzalez, J.A. Pople, Gaussian, Inc., Wallingford CT, 2004.
[19] S. Pshenichnyuk, N. Asfandiarov, V. Fal'ko, V. Lukin, Int. J. Mass Spectrom. 227 (2003) 259.
[20] R. Zenobi, R. Knochenmuss, Mass Spectrom. Rev. 17 (1998) 337.
[21] E. Nordhoff, A. Ingendoh, R. Cramer, A. Overberg, B. Stahl, M. Karas, F. Hillenkamp, Rapid Commun. Mass Spectrom. 6 (1992) 771.
[22] R. Knochenmuss, L.V. Zhigilei, J. Phys. Chem. B 109 (2005) 22947.
[23] S.N. Jackson, S. Mishra, K.K. Murray, J. Phys. Chem. B 107 (2003) 13106.

[24] F.H. Yassin, D.S. Marynick, J. Phys. Chem. A 110 (2006) 3820.
[25] R. Knochenmuss, Analyst 131 (2006) 966.
[26] M. Dashtiev, V. Frankevich, R. Zenobi, J. Phys. Chem. A 110 (2006) 926.
[27] S.A. Pshenichnyuk, N.L. Asfandiarov, Eur. J. Mass Spectrom. 10 (2004) 477.
[28] V. Karbach, R. Knochenmuss, Rapid Commun. Mass Spectrom. 12 (1998) 968.
[29] S.G. Lias, R.D. Levin, S.A. Kafafi, "Ion Energetics Data" in NIST Chemistry WebBook, in: P.J. Linstrom, W.G. Mallard (Eds.), NIST Standard Reference Database Number 69, National Institute of Standards and Technology, Gaithersburg MD, 20899, 2005, http://webbook.nist.gov.
[30] A.J. Hoteling, W.F. Nichols, D.J. Giesen, J.R. Lenhard, R. Knochenmuss, Eur. J. Mass Spectrom. 12 (2006) 345.
[31] R. Knochenmuss, Anal. Chem. 75 (2003) 2199.